Rare Metal Materials and Engineering
Volume 54, Issue 6, June 2025
Available online at www.rmme.ac.cn

Science Press

Cite this article as: Yan Jisen, Liu Kaixuan, Jin Fengyi, et al. Al and V Leaching Kinetics During Preparation of Ti6Al4V Alloy Powders by Multistage Deep Reduction Process[J]. Rare Metal Materials and Engineering, 2025, 54(06): 1426-1434. DOI: https://doi.org/10.12442/j.issn.1002-185X.20240356.

ARTICLE

Al and V Leaching Kinetics During Preparation of Ti6Al4V Alloy Powders by Multistage Deep Reduction Process

Yan Jisen[1,2], Liu Kaixuan[1,2], Jin Fengyi[1,2], Dou Zhihe[3], Zhang Tingan[3], Xie Fang[1,2], Hua Xijin[4]

[1] Henan Province Engineering Research Center of Additive Manufacturing Aeronautical Materials, Nanyang Institute of Technology, Nanyang 473004, China; [2] Nanyang Key Laboratory of Additive Manufacturing Technology and Equipment, Nanyang Institute of Technology, Nanyang 473004, China; [3] Key Laboratory for Ecological Metallurgy of Multimetallic Mineral, Ministry of Education, Northeastern University, Shenyang 110819, China; [4] Department of Engineering, University of Exeter, Exeter EX4 4QF, UK

Abstract: The leaching process of magnesiothermic self-propagating product generated during the multistage deep reduction process was investigated. The influence of magnesiothermic self-propagating product particle size, HCl solution concentration, and leaching solution temperature on the leaching behavior of elements Al and V was investigated. Results demonstrate that the leaching rate of Al and V is increased with the rise in leaching solution temperature, the increase in HCl solution concentration, and the enlargement of magnesiothermic self-propagating product particle size. The leaching processes of Al and V are consistent with the chemical reaction control model. When the magnesiothermic self-propagation product with D_{50} of 59.4 μm is selected as the raw material, the leaching temperature is 40 °C, and 1 mol/L HCl solution is employed, after leaching for 180 min, the leaching rates of Al and V are 24.8% and 12.6%, respectively. The acid-leached product exhibits a porous structure with a specific surface area of 3.5633 m^2/g.

Key words: multistage deep reduction process; Ti6Al4V alloy powder; acid leaching; magnesiothermic self-propagating

1 Introduction

Ti6Al4V alloy is a typical $\alpha+\beta$ type titanium alloy[1], which exhibits advantageous properties, including good biocompatibility, fine corrosion resistance, and nonmagnetic characteristics[2–3]. Currently, Ti6Al4V alloy is the most prevalent titanium alloy with a multitude of applications in medical, aircraft manufacturing, chemical, and other fields[4–7]. The continuous development of 3D printing technology[8–9], powder metallurgy technology[10–11], and selective laser melting technology[12–15] has led to an increase in the market demand for titanium alloy powder. Nevertheless, the high production cost exerts a significant barrier to the further expansion of titanium alloy applications.

Currently, the majority of titanium alloy powder is prepared by atomization technology. The first step in the production of titanium powder is the preparation of the titanium sponge, followed by the addition of alloying elements to the sponge for alloying and melting. Finally, the titanium alloy is atomized into powder by atomization technology[16]. The production of titanium sponges is a high-energy-consuming, polluting, and intermittent process. To reduce the production cost of titanium alloys, scholars have explored and developed different methods for the preparation of titanium alloy powder. Common methods are the electrochemical method and the metal thermal reduction method. Electrochemical methods involve preparation at the temperatures below the melting point of titanium alloys. The reduction temperatures of the metal thermal reduction method are usually below the melting point of titanium alloys. Even if the transient temperature exceeds the melting point of titanium alloys, it is still challenging to maintain the high temperature for a long

Received date: June 16, 2024
Foundation item: Scientific and Technological Project of Nanyang (23KJGG017); Key Specialized Research & Development and Promotion Project (Scientific and Technological Project) of Henan Province (232102221022); College Students and Technology Innovation Fund Project of Nanyang Institute of Technology (2023139); Project of Doctoral Scientific Research Startup Fund of Nanyang Institute of Technology (NGBJ-2023-25)
Corresponding author: Dou Zhihe, Ph. D., Professor, Key Laboratory for Ecological Metallurgy of Multimetallic Mineral, Ministry of Education, Northeastern University, Shenyang 110819, P. R. China, E-mail: douzh@smm.neu.edu.cn

period. Consequently, the electrochemical method and the metal thermal reduction method can maintain the intrinsic state of the raw materials, and titanium alloy powders can be obtained directly through the utilization of powdered raw materials.

The electrochemical method employs the principle of electron transfer, which entails a direct reduction of the cathode titanium dioxide to titanium metal or the titanium element at the anode being transformed into the ionic state in the molten salt. Thereafter, the titanium ions existing in the molten salt undergo reduction to titanium metal. A novel approach to the synthesis of titanium metal powders via molten salt electrolysis of TiO_2 was initially proposed in Ref. [17–18]. Subsequently, Suzuki[19–20], Park[21], Jiao[22], and Zhu[23] et al investigated this method and expanded the experimental estimation range to the scale of tens of kilograms. Nevertheless, the challenges of recycling the molten salt and the high production cost remain significant obstacles to overcome. The process of thermal metal reduction involves the removal of elemental oxygen from the feedstock through a metal with oxygen binding ability acting as the reducing agent. The conventional thermal metal reduction method employs Mg and Na as reducing agents to reduce $TiCl_4$ to obtain the titanium sponge. To reduce the addition of $CaCl_2$ in the electrochemical process, Okab et al[24] proposed the preform reduction process. TiO_2, $CaCl_2$, and CaO were mixed and sintered, and then the titanium powders with 99% purity could be obtained by Ca vapor reduction at 1073–1273 K for 6 h followed by acid leaching. Yang et al[25] enhanced the process-removal-product process by eliminating the pre-sintering step and reducing the reaction time. Nevertheless, the utilization rate of Ca vapor was found to be exceedingly low with a considerable quantity of Ca metal condensing on the upper part of the reactor after the reaction. To enhance the utilization rate of metallic Ca, Yan et al[26] conducted a direct mixing process involving small particle-sized metallic Ca powder with TiO_2, V_2O_5, and Al powder. This process resulted in the formation of Ti6Al4V powder through the self-propagating reaction. Nevertheless, metallic Ca is highly reactive, and the production of small particle metallic Ca powder is costly and unsuitable for preservation purpose. The production and storage costs of metallic Mg powder are lower than those of metallic Ca powder. Consequently, the utilization of metal Mg powder as a reducing agent can reduce the production cost. Sarkar et al[27] employed a novel reduction process involving TiO_2, $MgCl_2$, and Mg with the introduction of H_2 during the reduction. The use of hydrogen atoms to destabilize the Ti-O solid solution results in the production of low-oxygen titanium powder. Zhao et al[28–31] uniformly mixed Na_2TiF_6, NaF, and Al powder for reduction, resulting in the production of Ti powder, Ti_3Al powder, and TiAl powder. However, the product exhibited a high oxygen content and was therefore unsuitable for direct use.

To reduce the oxygen content in the product while lowering the production cost, Yan et al[32–34] proposed a new process for the preparation of Ti6Al4V alloy powders by multistage deep reduction. The Ti-Al-V-O precursor was initially obtained by the rapid thermal self-propagation reaction rate of Mg. To further reduce the oxygen content in the Ti-Al-V-O precursor, deep deoxidation was conducted at 1000–1300 K using metal Ca as a reducing agent. Nevertheless, the presence of MgO in the primary reduction product of magnesiothermic self-propagation process would impede the migration of oxygen atoms during the deep reduction process. Consequently, it was essential to eliminate MgO from the primary reduction product of magnesiothermic self-propagation. However, the dissolution of elements Ti, Al, and V into the HCl solution during the MgO removal process would result in a lack of product composition. Therefore, it is important to study the leaching mechanism of elements Ti, Al, and V during the dissolution of MgO in HCl solution. The leaching kinetics of the elements Mg and Ti have been previously reported in Ref.[35]. This research employed HCl solution as the leaching solvent to examine the impact of particle size, the concentration of HCl solution, and temperature of the leaching solution on the leaching process of elements Al and V in the primary reduction products of magnesiothermic self-propagating process.

2 Experiment

The Mg, TiO_2, V_2O_5, and Al powders were uniformly blended and subsequently compressed into lumps through cold pressing. These lumps were then placed in a self-propagating reactor. The gas within the reactor was replaced on three occasions with Ar gas, after which a resistance wire was employed to initiate the self-propagation reaction. The reaction products were crushed and then separated into four samples with particle size D_{50} of 85.3, 59.4, 50.9, and 26.7 μm. The HCl solutions of 1, 2, 3, and 4 mol/L were used as the leaching solution, and the leaching temperatures were selected as 30, 40, 50, and 60 °C.

To maintain a constant temperature throughout the experiments, the HCl solution of 2 L was placed in a three-necked flask before each experiment and stirred at a fixed speed of 250 r/min using a stirring paddle. The flask was maintained at a constant temperature through water bath for 30 min, after which 1.5 g magnesiothermic self-propagation product was added. Samples of 3–5 mL were taken out at 1, 3, 5, 7, 10, 15, 30, 45, 60, 90, 120, 150, and 180 min from the beginning of the experiment to ensure that the liquid-to-solid ratio of the experiment remained constant. The samples were then quickly filtered. The element concentrations of Al and V in solution were determined using inductively coupled plasma optical emission spectrometry (ICP-OES) with calibration. The specific experiment conditions are presented in Table 1.

The phase of the products was characterized by X-ray diffraction (XRD, Bruker, D8). The microstructure of the products was characterized by field-emission scanning electron microscope (SEM, SU8010, Hitachi) coupled with energy dispersive spectrometer (EDS). The specific surface area of the products was determined using a surface area analyzer (ASAP2020M). The concentrations of aluminum and

vanadium in the solution were analyzed by ICP-OES (Leeman, Prodigy XP).

The original morphologies of the magnesiothermic self-propagation product are illustrated in Fig. 1. According to Fig. 1a–1b, the original morphologies of the magnesiothermic self-propagation product show an amorphous lump with particles attached to the surface. Fig. 1c depicts the cross-sectional morphology of the magnesiothermic self-propagation product. It can be observed that the product can be internally divided into two distinct regions, which are characterized by dark and light grey hues. According to Fig. 1d, the dark grey part is primarily composed of elements Mg and O, whereas the light grey part is primarily composed of elements Ti, Al, and V. These two types of enriched areas are closely combined.

Fig. 2 illustrates XRD pattern of the magnesiothermic self-propagation product. As illustrated in Fig. 2, the composition of the phase in magnesiothermic self-propagation product is predominantly MgO and the low-valent oxides of titanium. The elements V and Al cannot be observed, and they exhibit a certain degree of solid solubility in Ti.

3 Results and Discussion

3.1 Leaching process of element Al

When the HCl solution concentration is 1 mol/L and the particle size D_{50} of the magnesiothermic self-propagation product is 85.3 μm, the variation curves of the leaching rate of the element Al are shown in Fig. 3. As shown in Fig. 3a, with the increase in the temperature, the leaching rate of element Al is increased. With the prolongation of leaching time, the leaching rate of Al is also increased. After leaching for 180 min, the leaching rate of Al in the systems with temperature of 30, 40, 50, and 60 °C is found to be 5.6%, 22.0%, 43.7%, and 66.2%, respectively. This result indicates that the increase in temperature is accompanied by a proportional increase in the loss of element Al from the product.

When the HCl solution concentration is 1 mol/L and the temperature is 40 °C, the variation curves of the leaching rate of element Al with the particle size of the magnesiothermic self-propagation product are shown in Fig. 3b. As illustrated in Fig. 3b, the leaching rate of Al exhibits a clear increase trend with the reduction in particle size of the raw material without

Table 1 Experiment conditions

No.	HCl solution concentration/mol·L^{-1}	Temperature/°C	Particle size, D_{50}/μm
1	1	30	85.3
2	1	40	85.3
3	1	50	85.3
4	1	60	85.3
5	1	40	59.4
6	1	40	50.9
7	1	40	26.7
8	2	40	59.4
9	3	40	59.4
10	4	40	59.4

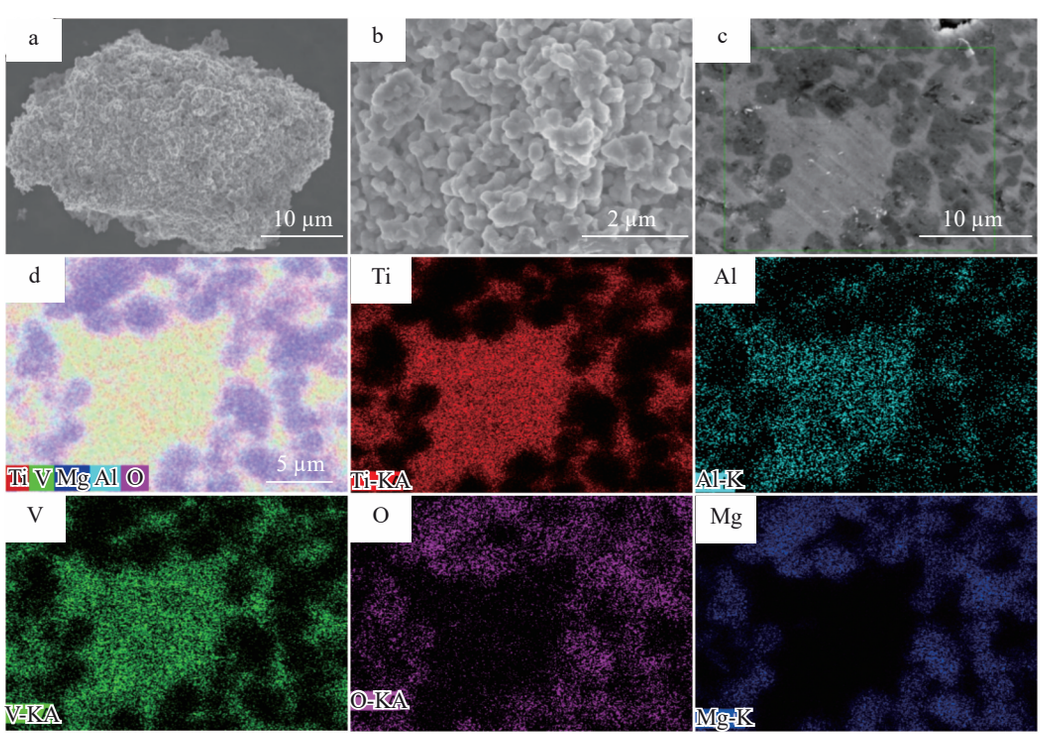

Fig.1 SEM morphologies (a–b) and cross-sectional morphology (c) of magnesiothermic self-propagation powder product; element distributions corresponding to green rectangular area in Fig.1c (d)

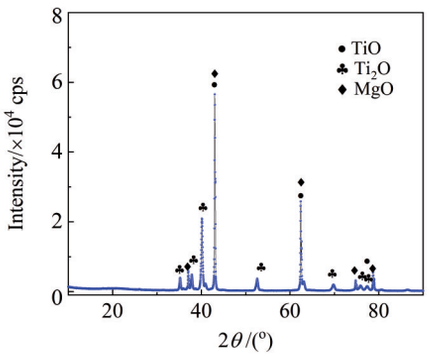

Fig.2 XRD pattern of magnesiothermic self-propagation product

discernible turning point. With the prolongation of leaching time, the leaching rate of Al is also increased. After leaching for 180 min, the leaching rate of Al reaches 22.0%, 24.8%, 25.6%, and 26.1% with particle sizes of 85.3, 59.4, 50.9, and 26.7 μm, respectively. This result suggests that the reduction in particle size of the magnesiothermic self-propagation primary reduction product is associated with the increase in the leaching rate of Al.

When the temperature of the leaching solution is 40 °C and the particle size D_{50} of the magnesiothermic self-propagation product particle size is 59.4 μm, the variation curves of the leaching rate of element Al with the HCl solution concentration are shown in Fig.3c. As illustrated in Fig.3c, the leaching rate of Al is increased with the increase in HCl solution concentration. With the prolongation of leaching time, the leaching rate of Al is also increased. After leaching for 180 min, the leaching rate of Al reaches 61.7%, 53.1%, 43.5%, and 24.8% with HCl solution concentrations of 4, 3, 2, and 1 mol/L, respectively. This result indicates that a high HCl solution concentration may result in a significant increase in the amount of Al loss during the acid-leaching process. This comparison of the effects of leaching solution temperature, magnesiothermic self-propagation product particle size, and HCl solution concentration on the leaching rate of Al reveals that the temperature and HCl solution concentration exert a significant influence on the leaching rate of Al. To minimize the loss of element Al, it is recommended to lower the leaching temperature and HCl solution concentration.

3.2 Leaching process of element V

When the concentration of the HCl solution is 1 mol/L and the particle size D_{50} of the magnesiothermic self-propagation product particle size is 85.3 μm, the variation curves of the leaching rate of element V with temperature and time are shown in Fig. 4a. Fig. 4a indicates that the leaching rate of element V is comparable to that of element Al. The leaching rate of element V is increased with the increase in temperature and the prolongation of leaching time. After leaching for 180 min, the leaching rate of V in the systems with temperatures of 30, 40, 50, and 60 °C is found to be 2.3%, 7.9%, 29.2%, and 51.0%, respectively. This result indicates that with the increase in temperature, the leaching rate of element V is increased in the product.

When the concentration of the HCl solution is 1 mol/L and the temperature is 40 °C, the variation curves of the leaching rate of element V with the particle size of the magnesiothermic self-propagation product and time are shown in Fig. 4b. As illustrated in Fig. 4b, a reduction in the particle size of the raw material is accompanied by an increase in the leaching rate of element V. With the prolongation of leaching time, the leaching rate of V is also increased. After leaching for 180 min, the leaching rate of V reaches 7.9%, 12.6%, 12.8%, and 13.6% with particle sizes of 85.3, 59.4, 50.9, and 26.7 μm, respectively. This result indicates that the reduction in particle size of the magnesiothermic self-propagating primary reduction product results in an increase in the amount of V loss.

When the temperature of the leaching solution is 40 °C and the particle size D_{50} of the magnesiothermic self-propagation product particle size is 59.4 μm, the variation curves of the leaching rate of element V with the HCl solution concentration and time are shown in Fig. 4c. As illustrated in Fig. 4c, the leaching rate of element V is increased with the increase in HCl solution concentration. With the prolongation of leaching time, the leaching rate of V is also increased. After leaching for 180 min, the leaching rate of V reaches 57.0%, 46.37%, 33.0%, and 12.6% with HCl solution concentrations of 4, 3, 2, and 1 mol/L, respectively. This result indicates that the increase in HCl solution concentration causes a significant increase in the leaching rate of V in the process of acid

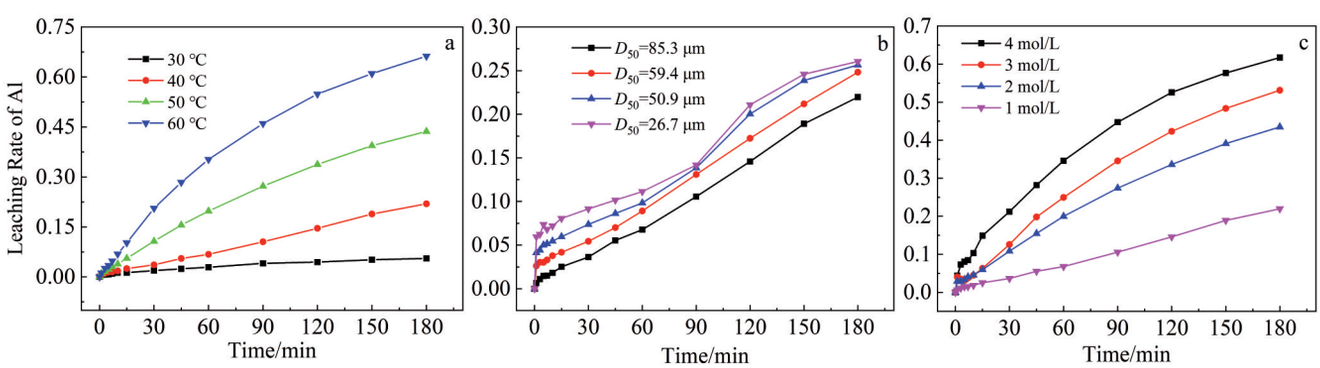

Fig.3 Influence of temperature (a), particle size (b), and HCl solution concentration (c) on leaching rate of element Al

leaching. The comparison of the effects of leaching solution temperature, magnesiothermic self-propagation product particle size, and HCl solution concentration on the leaching rate of elemental V reveals that the temperature and HCl solution concentration exert a significant influence on the leaching rate of element V. To prevent the loss of element V, it is recommended to lower the leaching temperature and HCl solution concentration.

3.3 Leaching kinetic analysis

To investigate the nature of the interaction of the elements Al and V with the HCl solution, leaching rate data at different temperatures were fitted using different reaction control models. The leaching of metallic elements from magnesiothermic self-propagation products is a solid-liquid non-homogeneous phase reaction. The reaction occurs at the surface of unreacted particles. In the process of continuous leaching, the reaction interface gradually contracts towards the interior of the particle, resulting in the formation of a porous structure. Consequently, the leaching kinetics are consistent with the unreacted shrinkage kernel model. These phenomena can be classified into three categories: chemical reaction control, internal diffusion control, and external diffusion control. The leaching kinetic models corresponding to chemical reaction control, internal diffusion control, and external diffusion control, as presented in Eq. (1 – 3) respectively, as follows:

$$1-(1-\alpha)^{1/3}=k_1t \quad (1)$$

$$1-2\alpha/3-(1-\alpha)^{2/3}=k_2t \quad (2)$$

$$1-(1-\alpha)^{2/3}=k_3t \quad (3)$$

where α is the leaching rate; t is time; k_1, k_2, and k_3 are constants.

Arrhenius equation is also required for calculation, as follows:

$$\ln k=B-E/RT \quad (4)$$

where k is the leaching rate constant; B is the intercept value of fitting line; E is the apparent activation value; R is the thermodynamic constant; T is the temperature.

Because the leaching rate constant k is a function of the HCl solution concentration C, it is necessary to consider the formula in Eq.(5), as follows:

$$\ln k=D+n\ln C \quad (5)$$

where D is the intercept value of fitting line; n is the number of reaction stages; C is the concentration of HCl solution.

To investigate the leaching kinetics of Al during the leaching process in HCl solution, the leaching rate data for the element Al were input into different kinetic functions for fitting analysis. The calculated results are shown in Table 2. It is found that the correlation coefficient R^2 of all data exceeds 0.97 when the chemical reaction control model is used for fitting. This result indicates that the leaching process of Al during the experiment is in accordance with the chemical reaction control model, as illustrated in Fig. 5a and 5c.

The relationship between ln$k$ and 1000/T can be observed in Fig. 5b. After linear fitting of the relevant data, the apparent activation value E of the reaction can be obtained. The apparent activation E of the Al leaching reaction is calculated to be 80.06 kJ/mol when the HCl solution concentration is 1 mol/L. The apparent activation E, derived from the Arrhenius formula, is greater than 41.8 kJ/mol, which indicates that the Al leaching process is in accordance with the chemical reaction control. According to Eq. (5), the relationship of ln$k$-ln$C$ can be obtained in Fig.5d. The number of reaction levels of the leaching reaction can be obtained by linear fitting of the relevant data. The slope of the fitted line in Fig. 5d represents the reaction order of Al leaching from the HCl solution. It can be calculated that the reaction order of Al leaching from HCl solution with different HCl solution concentrations is 0.937, which indicates that increasing the HCl solution concentration has a significant effect on the leaching rate of Al.

To investigate the leaching kinetics of V during the leaching process in HCl solution, the leaching rate data for the element V were input into different kinetic functions for fitting analysis. The calculated results are shown in Table 3. It is found that the correlation coefficient R^2 of all data exceeds 0.99 when the chemical reaction control model is used for fitting. This result indicates that the leaching process of V during the experiment is in accordance with the chemical reaction control model, as illustrated in Fig.6a and 6c.

The relationship between ln$k$ and 1000/T is shown in Fig. 6b. After linear fitting of the relevant data, the apparent activation E of the reaction can be obtained. The apparent activation E of the V leaching reaction is calculated to be 97.98 kJ/mol when the HCl solution concentration is 1 mol/L.

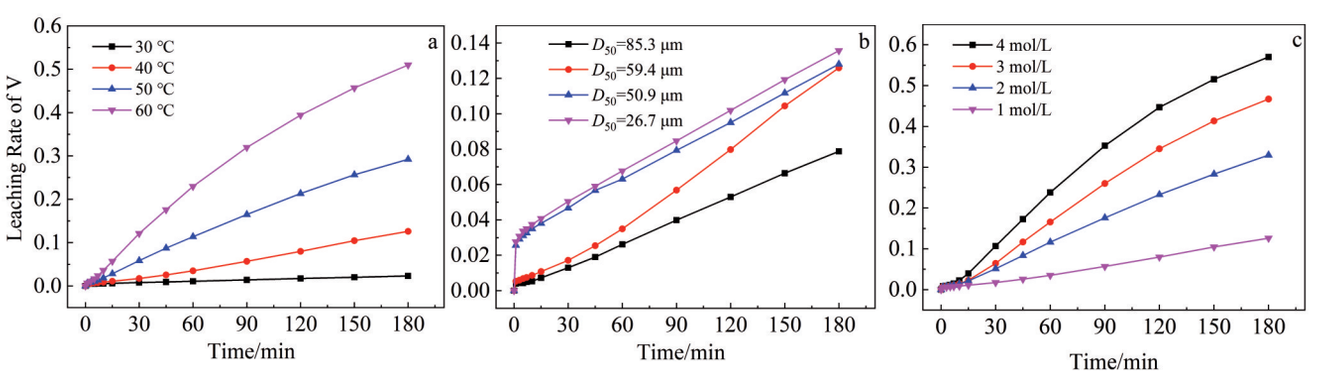

Fig.4 Influence of temperature (a), particle size (b), and HCl solution concentration (c) on leaching rate of element V

Table 2 Correlation coefficient R^2 of leaching rate of Al fitted under different kinetic models

Temperature/℃	HCl solution concentration/mol·L^{-1}	R^2		
		$1-(1-\alpha)^{1/3}$	$1-(1-\alpha)^{2/3}$	$1-2\alpha/3-(1-\alpha)^{2/3}$
30	1	0.987	0.959	0.992
40	1	0.997	0.965	0.901
50	1	0.997	0.990	0.968
60	1	0.993	0.992	0.985
40	2	0.994	0.990	0.902
40	3	0.992	0.986	0.972
40	4	0.972	0.965	0.991

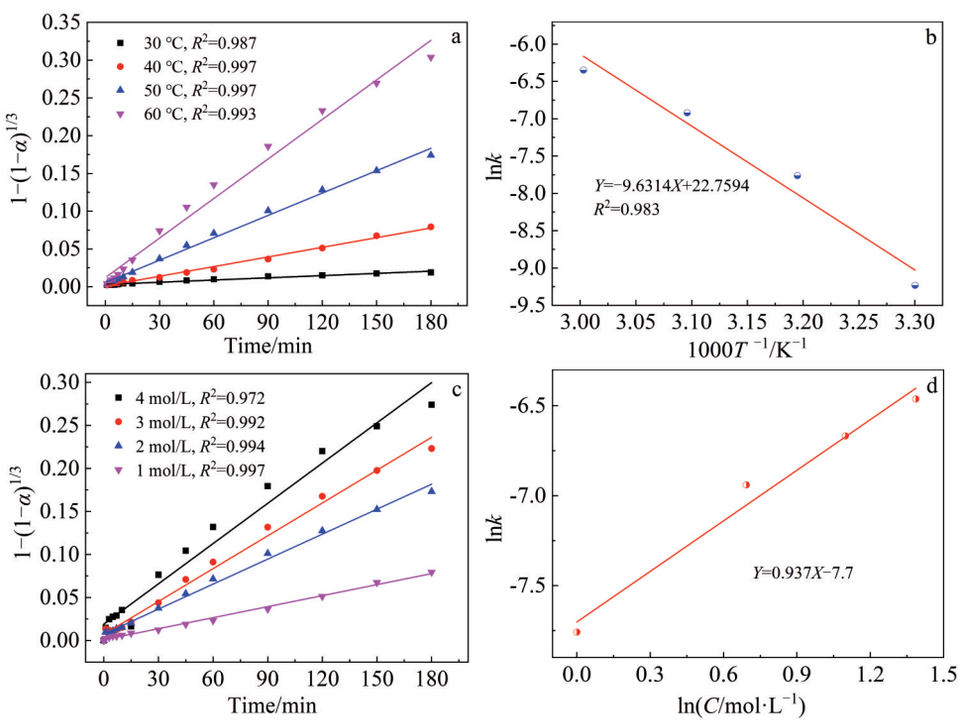

Fig.5 Relationship between $1-(1-\alpha)^{1/3}$ and time at different temperatures (a) and under different HCl solution concentrations (c) during Al leaching process; relationships of ln$k$-1000/T (b) and ln$k$-ln$C$ (d) during Al leaching process

Table 3 Correlation coefficient R^2 of leaching rate of V fitted under different kinetic models

Temperature/℃	HCl solution concentration/mol·L^{-1}	R^2		
		$1-(1-\alpha)^{1/3}$	$1-(1-\alpha)^{2/3}$	$1-2\alpha/3-(1-\alpha)^{2/3}$
30	1	0.999	0.966	0.971
40	1	0.995	0.990	0.880
50	1	0.999	0.997	0.946
60	1	0.998	0.980	0.965
40	2	0.999	0.998	0.925
40	3	0.996	0.995	0.930
40	4	0.996	0.992	0.953

The apparent activation E, derived from the Arrhenius formula, is greater than 41.8 kJ/mol, which indicates that the V leaching process is in accordance with the chemical reaction control model. According to Eq. (5), the relationship of ln$k$-ln$C$ is shown in Fig. 6d. The reaction order of the leaching reaction can be obtained by linear fitting of the relevant data. The slope of the fitted line in Fig. 6d represents the reaction order of V leaching from the HCl solution. It can be calculated that the reaction order of V leaching from HCl solution with different HCl solution concentrations is 1.3223,

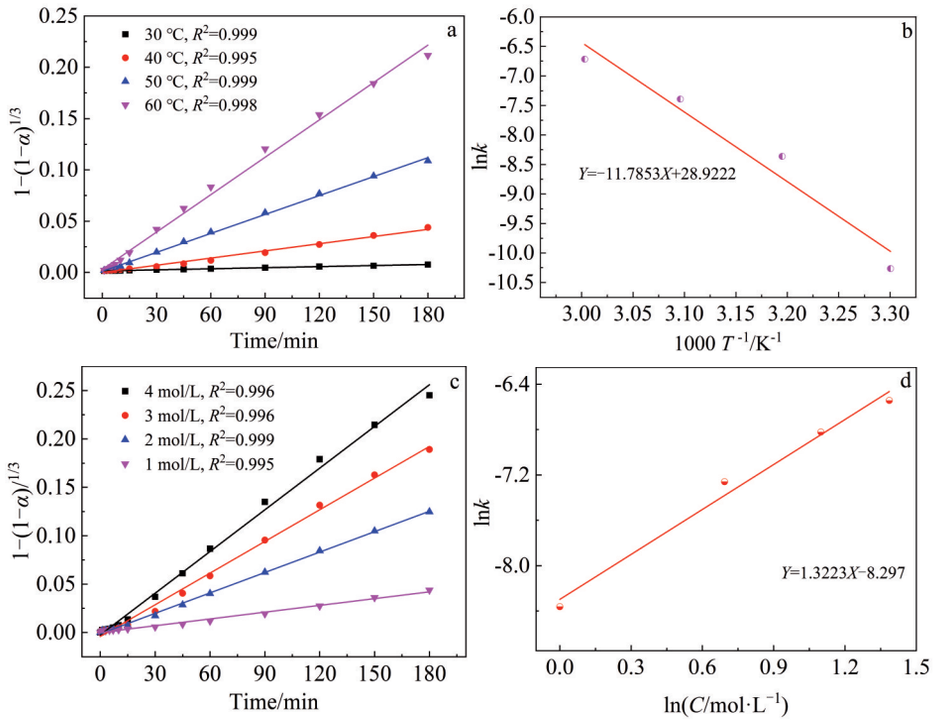

Fig.6 Relationship between $1-(1-\alpha)^{1/3}$ and time at different temperatures (a) and under different HCl solution concentrations (c) during V leaching process; relationships of ln$k$-1000/T (b) and ln$k$-ln$C$ (d) during V leaching process

which indicates that increasing the HCl solution concentration has a significant effect on the leaching rate of V.

3.4 Characteristics of product after acid leaching

The magnesiothermic self-propagating primary reduction product with the particle size D_{50} of 59.4 μm was employed as the raw material, and 1 mol/L HCl was used as the leaching solution for the following analysis. After leaching at 40 °C for 180 min, XRD and specific surface area analysis results of the leached product are presented in Fig. 7. As shown in Fig. 7a, the phase of the acid-leached product is predominantly composed of low-valent titanium oxides. Compared with the analysis from Fig. 2, the diffraction peaks of MgO disappear. Furthermore, the diffraction peaks of Al and V are absent in Fig.7a.

Fig. 7b illustrates that the adsorption and desorption curves of the acid-leached product exhibit characteristics consistent with class II adsorption isotherms, as defined by the International Union of Pure and Applied Chemistry (IUPAC) classification criteria. The adsorption curve exhibits a clear inflection point in the low-pressure section, indicating that monolayer adsorption has been completed at this point. Subsequently, multilayer adsorption occurs with the increase in partial pressure. A clear hysteresis can be observed in the desorption curve in the high-pressure area. This phenomenon can be attributed to the occurrence of capillary condensation between particles and within the macropores, which results in a hysteresis in the desorption curve. This result implies that the isotherms obtained at the time of desorption do not coincide with the isotherms obtained at the time of adsorption. The specific surface area of the product after acid leaching is

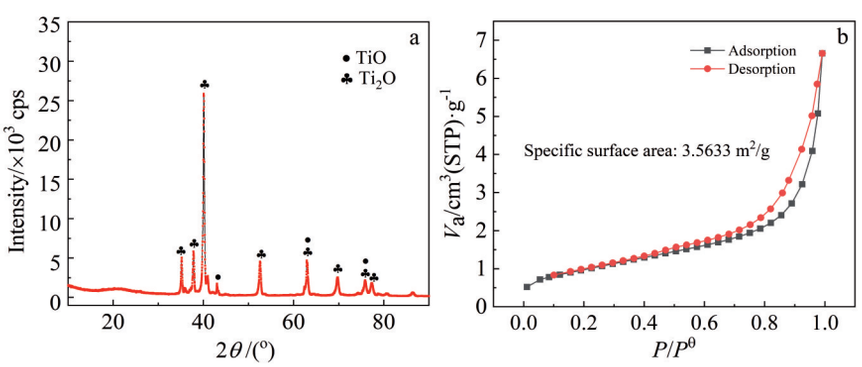

Fig.7 XRD pattern (a) and adsorption-desorption curves for N_2 (b) of products after acid leaching

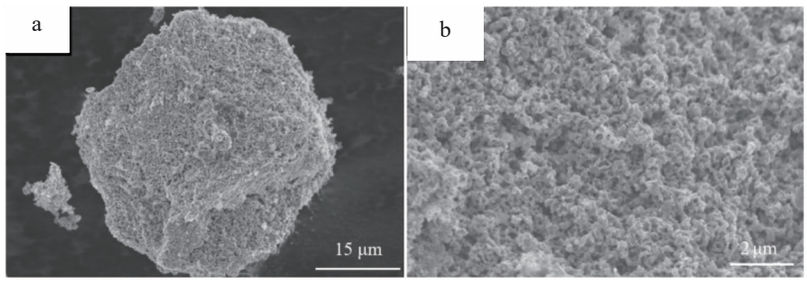

Fig.8 Morphologies of magnesiothermic self-propagation products

3.5633 m^2/g. Fig. 8a – 8b illustrate the morphologies of the product after acid leaching. It is revealed that the acid-leaching process results in the removal of MgO and the formation of a porous and loose product.

4 Conclusions

1) With the increase in leaching temperature, the increase in HCl solution concentration, and the decrease in raw material particle size, the leaching rates of Al and V are increased. The leaching process of both Al and V conforms to the chemical reaction control model.

2) The apparent activation *E* of the Al leaching reaction is calculated to be 80.06 kJ/mol when the HCl solution concentration is 1 mol/L. The reaction order for the leaching of Al with different HCl solution concentrations is found to be 0.937.

3) The apparent activation *E* of the leaching reaction of V is determined to be 97.98 kJ/mol. The reaction order for the leaching of V with different HCl solution concentrations is found to be 1.3223.

References

1 Zhou X F, Li Y L, Han Z R *et al*. *Journal of Alloys and Compounds*[J], 2023, 956: 170330

2 Sun R C, Mi G B, Huang X *et al*. *Modern Physics Letters B*[J], 2024, 38(4): S0217984923502639

3 Wang P F, Miao X J, Wu M P *et al*. *Journal of the Brazilian Society of Mechanical Sciences and Engineering*[J], 2024, 46(2): 79

4 Goyal V, Verma G. *Journal of Tribology-Transactions of the Asame*[J], 2024, 146(6): 4064506

5 Matysiak K, Jablonski P, Cholewa-Kowalska K *et al*. *Metallurgy and Materials Transactions A-Physical Metallurgy and Materials Science*[J], 2024, 55(3): 955

6 Zhai C C, Wang C M, Zhang M Y *et al*. *Materials Today Communications*[J], 2023, 37: 107363

7 Li M, Gupta A, Bennett C J *et al*. *International Journal of Mechanical Science*[J], 2023, 258: 108567

8 Subeshan B, Asmatulu E, Ma A T *et al*. *International Journal of Advanced Manufacturing Technology*[J], 2023, 129(11–12): 4939

9 Yoder J K, Erb D J, Henderson R *et al*. *Journal of Materials Processing Technology*[J], 2023, 322: 118201

10 Yadav B N, Lin D W, Lin M C *et al*. *Materials Letters*[J], 2024, 356: 135580

11 Koju N, Hermes J, Saghaian S E *et al*. *International Journal of Advanced Manufacturing Technology*[J], 2024, 130(3–4): 1495

12 Gülenç I T, Bai M W, Mitchell R L *et al*. *Journal of Rapid Prototyping*[J], 2024, 30(2): 378

13 Hua Z J, Hu Y Y, Mi G Y *et al*. *Vacuum*[J], 2024, 220: 112836

14 Rahmani R, Lopes S I, Prashanth K G *et al*. *Journal of Functional Biomaterials*[J], 2023, 14(10): 14100521

15 Singh S N, Deoghare A B. *Engineering Failure Analysis*[J], 2023, 148: 107208

16 Yan J S, Wang M H, Zhang T G *et al*. *Nano Technology Review* [J], 2024, 13(1): 20240016

17 Chen G Z, Fray D J, Farthing T W. *Cheminform*[J], 2010, 32(2): 361

18 Chen G Z, Fray D J, Farthing T W. *Metallurgy and Materials Trading B-Process Metallurgy and Materials Processing Science* [J], 2001, 32(6): 1041

19 Suzuki R O, Ono K, Teranuma K. *Metallurgical and Materials Transactions B*[J], 2003, 34(3): 287

20 Suzuki R O. *Journal of Physics and Chemistry of Solids*[J], 2005, 66(S2–S4): 461

21 Park I, Abiko T, Okabe T H, *Journal of Solid State Physical Chemistry*[J], 2005, 66(2–4): 410

22 Jiao S Q, Zhu, H M. *Journal of Alloys and Compounds*[J], 2007, 438(1–2): 243

23 Zhu H M, Jiao S Q, Xiao J S *et al*. *Extractive Metallurgy of Titanium*[M]. Amsterdam: Elsevier, 2020: 315

24 Okabe T H, Oda T, Mitsuda Y, *Journal of Alloys and Compounds* [J], 2004, 364(1–2): 156

25 Yang G B, Xu B Q, Lei X J *et al*. *Vacuum*[J], 2018, 157: 453

26 Yan J S, Dou Z H, Zhang T A. *Journal of Materials Research and Technology*[J], 2023, 27: 508

27 Sarkar S, Free M L, Benedict J *et al*. *Today Materials Today Chemistry*[J], 2020, 16: 100259

28 Zhao K, Wang Y W, Peng J P. *Rare Metals*[J], 2017, 36(6): 527

29 Zhao K, Feng N X, Wang Y W. *Intermetallics*[J], 2017, 85: 156

30 Zhao K, Gao F. *Journal of Alloys and Compounds*[J], 2021, 855(2): 157546

31 Zhao K, Wang Y W, Feng N X. *JOM*[J], 2017, 69(10): 1795
32 Yan Jisen, Dou Zhihe, Zhang Tingan. *Rare Metal Materials and Engineering*[J], 2022, 51(8): 2892 (in Chinese)
33 Yan Jisen, Dou Zhihe, Niu Liping *et al*. *Rare Metal Materials and Engineering*[J], 2021, 50(8): 2973 (in Chinese)
34 Yan Jisen, Dou Zhihe, Zhang Tingan *et al*. *Rare Metal Materials and Engineering*[J], 2021, 50(9): 3094
35 Yan Jisen, Dou Zhihe, Zhang Tingan. *Journal of Northeastern University* (*Natural Science*)[J], 2023, 44(10): 1416 (in Chinese)

多级深度还原法制备Ti6Al4V合金粉体过程中Al和V的浸出动力学

闫基森[1,2]，刘凯旋[1,2]，靳奉铱[1,2]，豆志河[3]，张廷安[3]，解　芳[1,2]，华细金[4]
(1. 南阳理工学院 河南省增材制造航空材料工程研究中心，河南 南阳 473004)
(2. 南阳理工学院 南阳市增材制造技术与装备重点实验室，河南 南阳 473004)
(3. 东北大学 多金属共生矿生态化冶金教育部重点实验室，辽宁 沈阳 110819)
(4. 埃克塞特大学 工程系，英国 埃克塞特 EX4 4QF)

摘　要：对多级深度还原法中镁热自蔓延产物的浸出过程进行了研究，探究了镁热自蔓延产物的粒度、浸出过程中盐酸溶液的浓度和浸出溶液温度对Al和V元素浸出行为的影响规律。结果表明，随着浸出溶液温度的升高、盐酸溶液浓度的增加和原料粒度的减小，相同时间内Al和V元素的浸出率增加。Al和V元素的浸出过程均符合化学反应控制模型。使用D_{50}为59.4 μm的镁热自蔓延产物作为原料，浸出温度40 ℃和1 mol/L的盐酸溶液作为浸出条件时，经过180 min的浸出，Al和V元素的浸出率分别为24.8%和12.6%。酸洗后的产物为多孔结构，比表面积为3.5633 m^2/g。

关键词：多级深度还原法；Ti6Al4V合金粉体；酸洗；镁热自蔓延

作者简介：闫基森，男，1993年生，博士，讲师，南阳理工学院河南省增材制造航空材料工程研究中心，河南 南阳 473004，E-mail：3011111@nyist.edu.cn